The Predictive Power of Computational Astrophysics as a Discovery Tool
Proceedings IAU Symposium No. 362, 2023
D. Bisikalo, D. Wiebe & C. Boily, eds.
doi:10.1017/S1743921322002319

3D Realistic Modeling of Solar-Type Stars to Characterize the Stellar Jitter

Irina Kitiashvili[1], Samuel Granovsky[1,2,3], Alan Wray[1]

[1]NASA Ames Research Center
Moffett Field, MS 258-6, Mountain View, CA, USA
email: irina.n.kitiashvili@nasa.gov, alan.a.wray@nasa.gov

[2]New Jersey Institute of Technology
323 Dr Martin Luther King Jr Blvd, Newark, NJ, USA
email: sg2249@njit.edu

[3]Universities Space Research Association
7178 Columbia Gateway Drive, Columbia, MD, USA

Abstract. Detection of Earth-mass planets with the radial velocity method requires a precision of about 10cm/s to identify a signal caused by such a planet. At the same time, noise originating in the photospheric and subphotospheric layers of the parent star is of the order of meters per second. Understanding the physical nature of the photospheric noise (so-called stellar jitter) and characterizing it are critical for developing techniques to filter out these unwanted signals. We take advantage of current computational and technological capabilities to create 3D realistic models of stellar subsurface convection and atmospheres to characterize the photospheric jitter. We present 3D radiative hydrodynamic models of several solar-type target stars of various masses and metallicities, discuss how the turbulent surface dynamics and spectral line characteristics depend on stellar properties, and provide stellar jitter estimates for these stars.

Keywords. stars: individual (HD209458); line: profiles; techniques: radial velocities, spectroscopic; methods: numerical

1. Introduction

Since the discovery of the first exoplanetary system, thousands of planets have been detected near other stars. However, the detection of Earth-mass planets remains a challenging task because the radial velocity variations due to the planetary motion are about ten cm/s, whereas the stellar disturbances are often order m/s (e.g., Plavchan et al. 2015; Fischer et al. 2016). The problem is complicated because stellar surface disturbances (so-called stellar jitter) arise from multiple physical processes. Several approaches to estimate stellar jitter have been developed, such as least-squares deconvolution (Bellotti et al. 2022), scaling relations (Luhn et al. 2020), and others. These methods allow us to investigate the dependence of stellar perturbations on metallicity, age, mass, magnetic activity, and evolutionary stage (e.g., Bastien et al. 2016; Meunier et al. 2017; Oshagh et al. 2017; Collier Cameron et al. 2021; Sowmya et al. 2021).

To characterize stellar jitter, we use existing computational capabilities to perform 3D radiative models of stellar convection and use the resulting models of atmospheres to compute synthetic spectra. This approach has been used to investigate stellar surface

Table 1. Stellar parameters used to generate 3D radiative models.

Star	Mass	Teff	log(g)	FeH
HD25171	1.08	6166	4.329	−0.032
HD49674	1.00	5598	4.408	0.126
HD69830	0.87	5383	4.469	0.038
HD121504	1.18	6071	4.355	0.236
HD209458	1.05	6095	4.314	−0.144

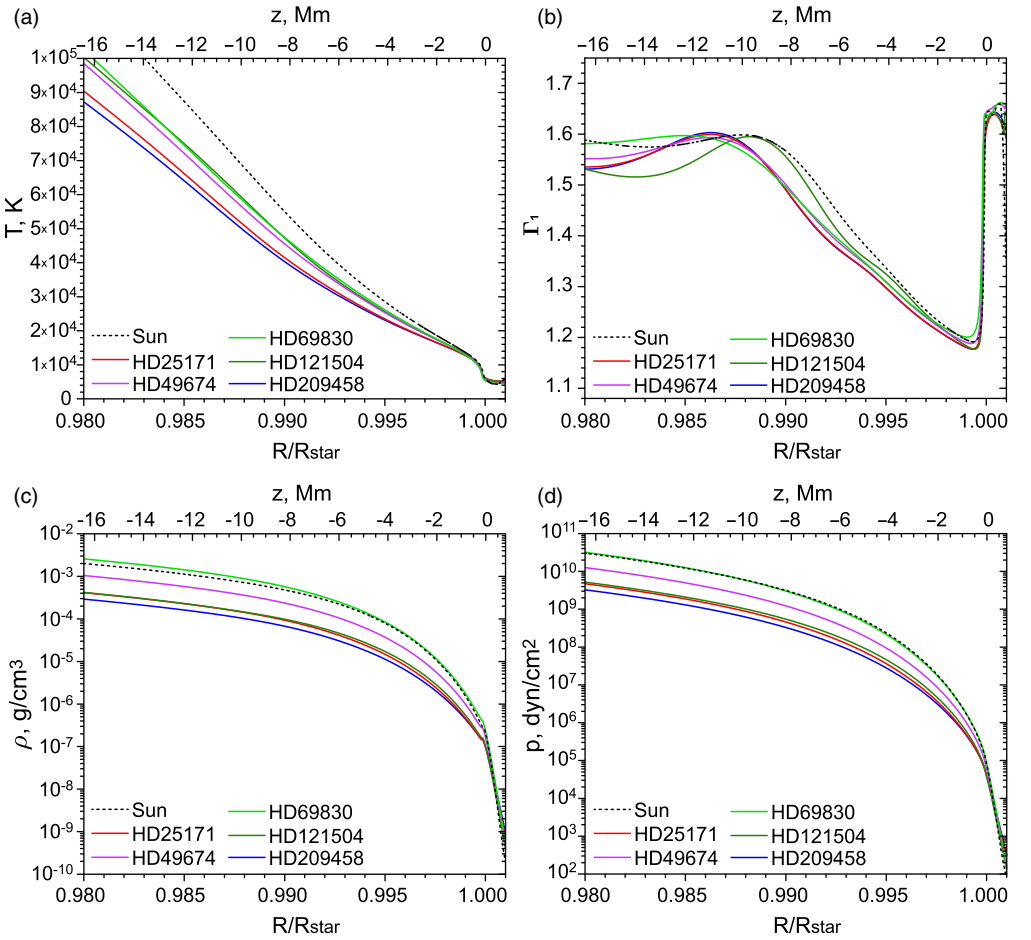

Figure 1. Internal structure of target stars obtained with the MESA code: a) temperature, b) adiabatic exponent, c) density, and gas pressure.

effects by various authors (e.g., Cegla et al. 2012, 2013; Dravins et al. 2017, 2021a,b). The present work presents initial results of modeling several target stars and computing spectral line syntheses over the stellar disks to investigate the jitter properties.

2. Computational setup to model stellar convection

To understand the nature of stellar jitter, we select five solar-type stars to characterize photospheric disturbances (Table 1). All these stars host Jupiter-size planets detected with the radial velocity method and are used as a testbed to investigate how different approaches to filtering out jitter signals can improve the signal quality of the radial

https://doi.org/10.1017/S1743921322002319 Published online by Cambridge University Press

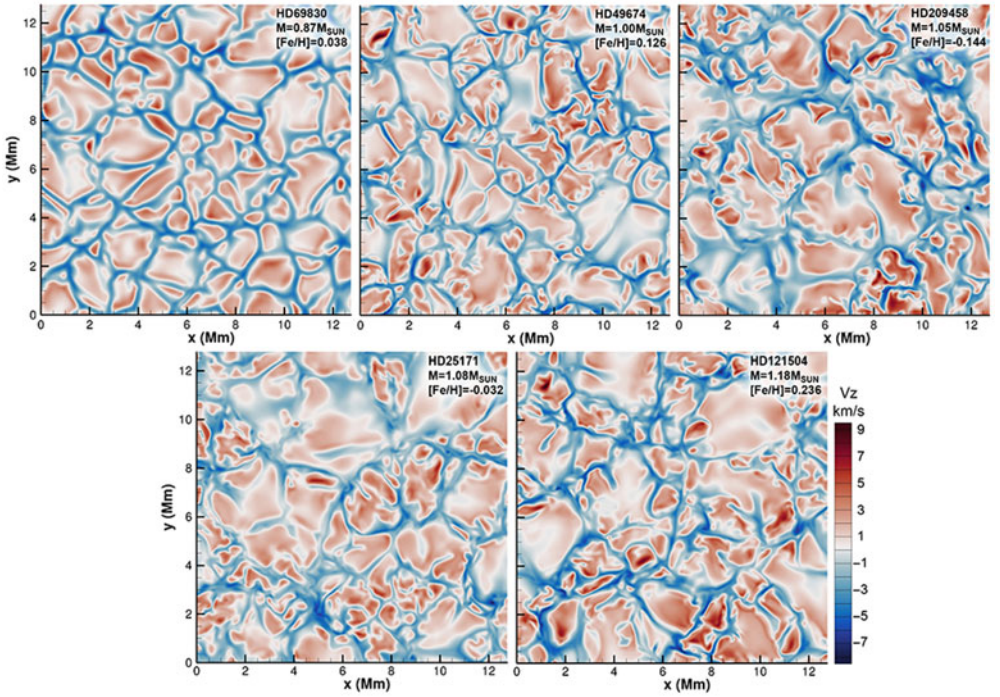

Figure 2. Granular structures at the photosphere reveal increased radial velocity amplitudes for more massive stars.

velocity residuals. As initial conditions, we use 1D mixing-length models of the stellar interiors (Fig. 1) generated with the MESA code (Paxton et al. 2011) in agreement with previously published stellar properties.

The 3D radiative hydrodynamics models of stellar convection are calculated using the StellarBox code (Wray et al. 2015, 2018). The radiative transfer calculations in this code are performed in the LTE approximation for four spectral bins; ray-tracing for 18 directional rays (Feautrier 1964) is implemented using the long-characteristics method. In this paper, we mostly consider time series obtained from simulations with 50 km grid resolution in the horizontal directions and, in the radial direction, varying from 20 km at the photosphere to 95 km near the bottom boundary of the computational domain. All models are computed for a 12.8 Mm-wide computational domain and cover 12 Mm of the convection zone and 1 Mm of atmosphere. The boundary conditions are periodic in the horizontal directions. No rotation is imposed.

3. Dynamics of the stellar convection

As stated above, we selected five target stars to to examine the properties of star-induced disturbances. Figure 1 shows the distribution of the radial (or vertical) component of velocity at the stellar photosphere for the target stars and the Sun. The photospheric structure for all stars reveals granulation patterns, including granules and mini-granules. These two populations of granular convection structures have been previously found in solar observations (Abramenko et al. 2012). However, the existence of the two populations is more prominent for more massive stars (Wray et al. 2015, 2018; Kitiashvili et al. 2016).

To investigate photosphere-originated disturbances, we synthesize six neutral iron lines (Fe I) at different locations on the stellar disk. The line profiles are used to examine the

https://doi.org/10.1017/S1743921322002319 Published online by Cambridge University Press

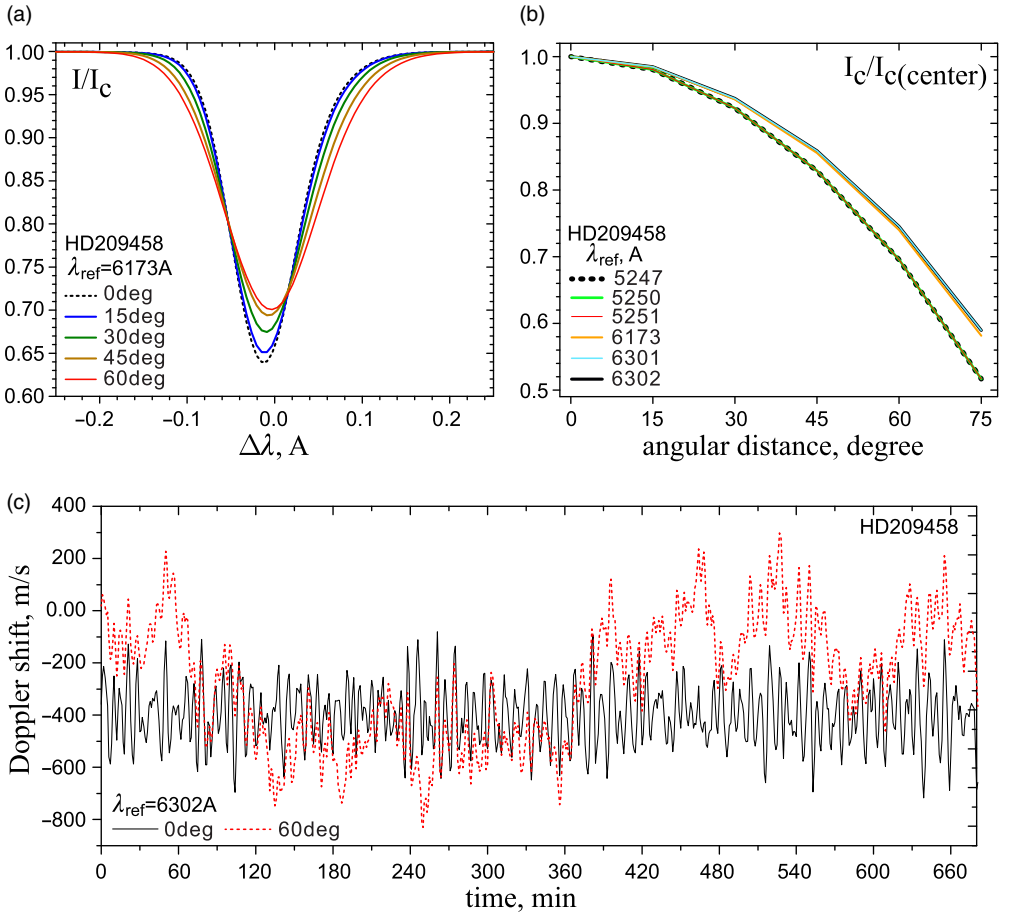

Figure 3. Center-to-limb effects: a) changes in the spectral line ($\lambda_{\rm ref} = 6173$Å) at different distances from the disk center; b) limb darkening profiles for six FeI lines; c) Doppler shift variations as a function of time at the stellar disk center (black solid curve) and at 60 degrees to limb (red dotted curve).

dependence of the Doppler shift disturbances on wavelength and distance from the disc center. The spectral line synthesis is performed in the LTE approximation with the Spinor code (Frutiger et al. 2000) using stellar atmosphere models from the 3D simulations.

Synthesis of the spectral lines for different distances from the stellar disk center allows us to investigate the dependence of line properties on their location relative to the disk center. Increasing the distance from the disk center causes an increase in line width and a decrease in the line depth and continuum intensity (Fig. 3 a, b). The resulting limb darkening profiles of modeled spectral lines are clustered in two groups, shorter and longer wavelengths (panel b). Because of the difference in the line formation height, each line probes a specific range of the atmospheric layers. For instance, in the case of a patch location closer to the limb, the light is integrated over a thicker column of the atmosphere and thus is more strongly affected by flows above the photosphere. Figure 3c shows time-variations of the Doppler shift, integrated over the computational domain at the disk center (black solid curve) and at 60 degrees longitude (red dotted curve). Because of the effect of horizontal flows, the Doppler shift can also vary significantly with time.

https://doi.org/10.1017/S1743921322002319 Published online by Cambridge University Press

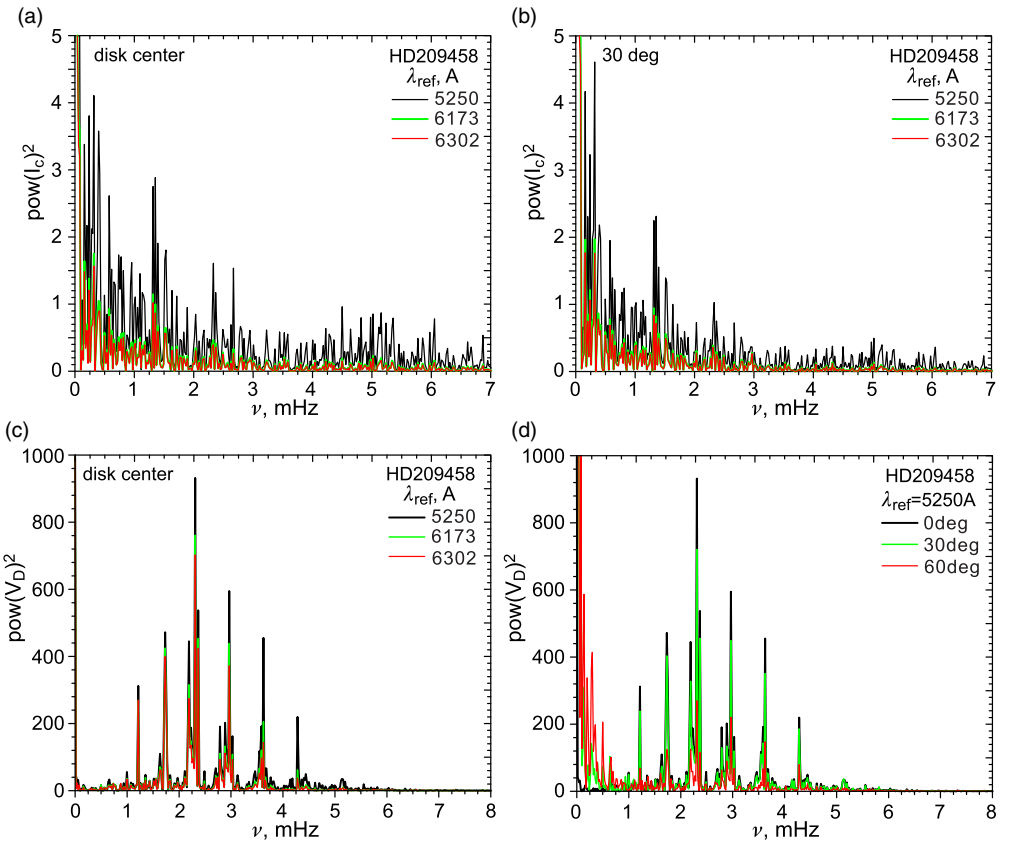

Figure 4. The power spectral density obtained from synthetic spectra of star HD209458. The power spectral density of the continuum intensity is shown for the disc center (panel a) and at 30 degrees longitude (panel b). The power spectral density of the Doppler-shift corresponds to the disc center of the simulated continuum intensity (panels a and b) and the Doppler-shift (panels c and d) at the disk center computed from three spectral lines (panel c), and for three distances from the disk center (0, 30, and 60 degrees) for one line (5250Å). In panels a-c, the power spectral density was obtained from synthesized data of three FeI lines: 5250Å (black curve), 6173Å (green), and 6302Å (red).

It is essential to note that the oscillatory properties depend on characteristics of the stellar convection, such as the size and lifetime of granulations, magnetic field flux and topology, etc. In the case of the hydrodynamic simulations presented in this paper, the properties of the stellar oscillations primarily depend on the distance from the disc center. Figure 4 shows a comparison of the power spectral density for the continuum intensity and the Doppler shift for three FeI lines. In particular, the power spectra of the continuum intensity show that the power decreases for longer wavelengths (Fig. 4a,b), which likely corresponds to a difference in the line formation heights. It is also confirmed by a decrease in the spectral density power of the Doppler shift at the disk center (panel c). Because radial motions are the main contributors to the signal, the continuum intensity (panel b) and Doppler shift oscillations are significantly reduced in the regions closer to the stellar limb.

https://doi.org/10.1017/S1743921322002319 Published online by Cambridge University Press

4. Discussion and conclusions

We presented initial results of modeling solar-type stellar dynamics to investigate the nature of stellar jitter and to develop data-characterization and filtering techniques for robust detection of Earth-mass exoplanets. We performed 3D radiative hydrodynamic simulations of stellar convection and computed synthetic spectroscopic observables of target stars. We used the model of planet-hosting star HD209458 for a detailed study. We demonstrated the capabilities of this approach to capture a variety of known effects, such as limb darkening and the dependence of spectral-power density on wavelength and location on the stellar disk.

Our current effort is to produce a series of high-resolution hydrodynamic and MHD models and develop a pipeline for efficient generation of time-dependent synthetic observables, data analysis, and investigation of different techniques for filtering the photospheric disturbances in spectroscopic observations of stellar jitter.

Acknowledgment

The work is supported by the NASA Extreme Precision Radial Velocity Foundation Science Program.

References

Abramenko, V. I., Yurchyshyn, V. B., Goode, P. R., Kitiashvili, I. N., & Kosovichev, A. G. 2012, ApJ, 756, L27
Bastien, F. A., Stassun, K. G., Basri, G., & Pepper, J. 2016, ApJ, 818, 43
Bellotti, S., Petit, P., Morin, J., et al. 2022, A&A, 657, A107
Cegla, H. M., Shelyag, S., Watson, C. A., & Mathioudakis, M. 2013, ApJ, 763, 95
Cegla, H. M., Watson, C. A., Marsh, T. R., et al. 2012, MNRAS, 421, L54
Collier Cameron, A., Ford, E. B., Shahaf, S., et al. 2021, MNRAS, 505, 1699
Dravins, D., Ludwig, H.-G., Dahlén, E., & Pazira, H. 2017, A&A, 605, A91
Dravins, D., Ludwig, H.-G., & Freytag, B. 2021a, A&A, 649, A16
Dravins, D., Ludwig, H.-G., & Freytag, B. 2021b, A&A, 649, A17
Feautrier, P. 1964, Comptes Rendus Academie des Sciences (serie non specifiee), 258, 3189
Fischer, D. A., Anglada-Escude, G., Arriagada, P., et al. 2016, PASP, 128, 066001
Frutiger, C., Solanki, S. K., Fligge, M., & Bruls, J. H. M. J. 2000, A&A, 358, 1109
Kitiashvili, I. N., Kosovichev, A. G., Mansour, N. N., & Wray, A. A. 2016, ApJ, 821, L17
Luhn, J. K., Wright, J. T., Howard, A. W., & Isaacson, H. 2020, AJ, 159, 235
Meunier, N., Mignon, L., & Lagrange, A. M. 2017, A&A, 607, A124
Oshagh, M., Santos, N. C., Figueira, P., et al. 2017, A&A, 606, A107
Paxton, B., Bildsten, L., Dotter, A., et al. 2011, ApJS, 192, 3
Plavchan, P., Latham, D., Gaudi, S., et al. 2015, arXiv e-prints, arXiv:1503.01770
Sowmya, K., Nèmec, N. E., Shapiro, A. I., et al. 2021, ApJ, 919, 94
Wray, A. A., Bensassi, K., Kitiashvili, I. N., Mansour, N. N., & Kosovichev, A. G. 2015, arXiv e-prints, arXiv:1507.07999
Wray, A. A., Bensassiy, K., Kitiashvili, I. N., Mansour, N. N., & Kosovichev, A. G. 2018, Realistic Simulations of Stellar Radiative MHD, ed. J. P. Rozelot & E. S. Babayev, 39